Center-to-limb darkening effect on spectral lines: typical cases of g-type stars

Fabrice BADO[1, 2*], Zacharie Sié KAM[1], Nekolgne Aymard BADOLO[1, 2], Baguima Gilbert BAYALA [1, 2], Jean KOULIDIATI[1]

Abstract

We present the impact of center-to-limb darkening (ε_i) on spectral line profiles of G-type stars through systematic analysis of cross-correlation function broadening. Using solar-type stellar spectra, we examine how center-to-limb darkening coefficients affect the measured full width at half maximum ($FWHM_{CC}$) and derived rotational velocities (V_{broad}). Our analysis employs the darkening coefficients from (Claret, 2000) and samples 19 rotational velocities from 0 to 100 km/s to optimize coverage of the observed stellar rotational ranges for calibration. We demonstrate that center-to-limb darkening variations induce systematic changes in measurements, with particularly pronounced effects for slow rotators where macroturbulence contributions (2-4 km/s) become dominant. The broadening parameter shows significant correlation with the darkening coefficient varying by 4.4 km/s (44.8%) over the studied range. These results highlight the critical importance of accurate center-to-limb darkening modeling for precise stellar rotation measurements in spectroscopic surveys of G-type stars.

Keywords *: Line broadening – Center-to-limb darkening – G-type stars*

Effet de l'assombrissement centre-bord sur les raies spectrales:

[1] Université Jospeh KI-ZERBO, Departement de Physique, Laboratoire de Physique et de Chimie de l'Environnement, 03 BP 7021, Ouagadougou, Burkina Faso
[2] Université Côte d'Azur, Observatoire de la Côte d'Azur, CNRS, Laboratoire Lagrange, Nice, France
*** Corresponding author** : Fabrice BADO, email : fabrice.bado@ujkz.bf / fabricebado726@gmail.com , ORCID : https://orcid.org/0000-0001-9696-6376

DOI : https://doi.org/10.64707/revstsna.v44i2.1830

Cas typique des étoiles de type G

Résumé

Nous présentons l'impact de l'assombrissement centre-bord (ε_i) sur les profils de raies spectrales des étoiles de type G à travers une analyse systématique de l'élargissement de la fonction de corrélation croisée. En utilisant des spectres stellaires de type solaire, nous examinons comment les coefficients d'assombrissement centre-bord affectent la largeur à mi-hauteur mesurée ($FWHM_{CC}$) et les vitesses de rotation dérivées (V_{broad}). Notre analyse utilise les coefficients d'assombrissement de (Claret, 2000) et échantillonne 19 vitesses de rotation de 0 à 100 km/s afin d'optimiser la couverture des plages de rotation stellaire observées pour l'étalonnage. Nous démontrons que les variations d'assombrissement centre-bord induisent des changements systématiques dans les mesures, avec des effets particulièrement prononcés pour les rotateurs lents où les contributions de macroturbulence (2-4 km/s) deviennent dominantes. Le paramètre d'élargissement montre une corrélation significative avec le coefficient d'assombrissement variant de 4,4 km/s (44,8%) sur la plage étudiée. Ces résultats soulignent l'importance critique d'une modélisation précise de l'assombrissement centre-bord pour des mesures exactes de la rotation stellaire dans les relevés spectroscopiques d'étoiles de type G.

Mots-clés : Élargissement de raie – Assombrissement centre-bord – Étoiles de type G

Introduction

Stellar center-to-limb darkening (which we denote ε_i), a well-established phenomenon in photometry and spectroscopy (Howarth, 2011; Manduca *et al*., 1977), exerts a considerable but often underestimated influence on the formation and observation of spectral lines (Collins and Truax, 1995; Espinoza and Jordán, 2015). This complex interaction between the spatial distribution of intensity across the stellar disk and line formation processes reveals fundamental aspects of stellar atmosphere physics, particularly critical for solar-type stars (Aufdenberg *et al.*, 2005; Hayek *et al.*, 2012).

This center-to-limb darkening describes the variation of observed luminous intensity from the center of the stellar disk toward its edge. This variation results from the angular dependence of radiative transfer

in the stellar atmosphere, where rays emitted from the limb traverse a greater optical depth through cooler and less dense atmospheric layers (Claret, 2000; Gray, 2008). The limb corresponds to regions where the observer's line of sight is tangential to the stellar surface (photosphere), as opposed to the disk center where it is perpendicular. G-type stars, characterized by effective temperatures between 5200 K and 6000 K, constitute a stellar class of major interest for modern astrophysics. They are also characterized by external convective atmospheres, favoring the formation of numerous metallic lines. Their proximity to solar parameters makes them privileged laboratories for studying stellar atmospheric processes (Gray, 2008). The parameterization of these stars and the precise determination of rotational broadening underscore the importance of a detailed understanding of their spectral properties (Doyle *et al.*, 2014).

In these stars, center-to-limb darkening results from temperature and density variations in the stellar atmosphere (Claret, 2000). The central regions of the disk, observed along a line of sight perpendicular to the surface, probe deeper and hotter atmospheric layers, while the limb regions, observed tangentially, preferentially sample the cooler superficial layers (Gray, 2008). This observational geometry induces significant spatial variations in local physical conditions, directly influencing line formation processes. Traditional spectroscopic analyses, based on spectra integrated over the entire stellar disk, can be affected by systematic biases if the center-to-limb darkening effect is not properly accounted for. These biases can lead to errors in the determination of effective temperature, surface gravity, and elemental abundances, etc.

The influence of center-to-limb darkening on spectral lines is of particular importance in several domains of stellar astrophysics: determination of stellar parameters, radial velocities, and rotational broadening. We present the impact of center-to-limb darkening on spectral line profiles of G-type stars through systematic analysis of cross-correlation (CC) function broadening (Claret, 2000; Gray, 2008). The aim of this article is to present the impact of center-to-limb

darkening on line profiles. The data and reduction are presented in Sect.I. The methodology adopted to determine the rotational velocity is presented in Sect.I. It relies on the determination of a coupling constant (A) between spectral line width and stellar rotation. The effect of the center-to-limb coefficient is presented in Sect.III and in Sect.IV we discuss the results. Finally, we summarizes our work.

I. Adopted methodology for measuring stellar rotational velocities

1. AMBRE synthetic spectra

For our study, we adopted the high-resolution AMBRE (Archéologie avec Matisse Basée sur les aRchives de l'ESO) synthetic spectra (de Laverny *et al.*, 2012). These theoretical spectra were generated from the MARCS stellar atmosphere model (Gustafsson *et al.*, 2008), recognized for its precision in modeling the outer layers of stars. This model sophisticatedly integrates the complex physical processes that govern the structure and dynamics of stellar atmospheres, including the effects of radiative opacity, convection, and hydrostatic equilibrium. This approach not only allows the most faithful possible reproduction of the thermodynamic conditions prevailing in stellar atmospheres but also and above all enables the prediction of observable spectral characteristics with high precision.

The AMBRE synthetic spectra cover a wavelength range from 300 nm to 1200 nm, with a spectral step of 0.001 nm (i.e., a total of 900,000 pixels). The adopted step corresponds to a spectral resolution ($R = \lambda/\Delta\lambda$) exceeding 150,000 in the ultraviolet domain, and on the order of 600,000 in the near infrared. In order to allow simple and rapid spectral adaptation to the properties of any spectrograph or other scientific applications, the AMBRE synthetic spectra were generated without undergoing prior convolution. In this way, it was possible to more easily degrade these spectra to adapt them to the characteristics of the FEROS spectrograph (see section 2.3). The initial synthetic spectra, generated at high spectral resolution, underwent no prior instrumental

convolution, thus preserving all the intrinsic physical information of the atmosphere model. To compare them with observations, we degraded these spectra by convolving them with an instrumental transfer function representative of the spectral resolution of FEROS (Fiberfed Extended Range Optical Spectrograph). This operation, which simulates the instrumental broadening of lines, induces irreversible information loss, but allows homogenization of theoretical and observed data.

2. Observed Solar Spectrum

We use the real solar spectrum in the context of this work. This spectrum comes from the BASS2000 (BAse de données Solaire Sol) observational database[3] which is dedicated to archiving and disseminating solar observational data. This database therefore combines observations from ground based instruments (Jungfraujoch, Kitt Peak) and space-based instruments – SOHO (Solar and Heliospheric Observatory)/SUMER (Solar Ultraviolet Measurements of Emitted Radiation, (Curdt, 2001)) – to cover the entire solar electromagnetic spectrum. It is managed by the Paris Observatory and is part of the Laboratoire d'Études Spatiales et d'Instrumentation en Astrophysique (LESIA). The presented solar spectrum comes from several ATLAS observations (Automatic Telescope for Limb and Active Sun) and the main instruments used depend on the spectral domains:

- Ultraviolet (670 Å to 1609 Å): SUMER instrument aboard the SOHO mission (resolution 0.04 Å)
- Visible (3000 Å to 10000 Å): observations carried out from the Jungfraujoch observatory, resolution 0.002 Å or 500 pixels/Å) corresponding to a resolution R between $1{,}5\times10^6$ and 5×10^6, which corresponds to very high spectral (instrumental) resolution, typical of instruments used for precision solar spectroscopy.

3 See https://bass2000.obspm.fr/solar_spect.php.

- Infrared (10000 Å to 54000 Å): observations carried out from the Kitt Peak observatory[4] (resolution 0.004 cm^{-1}, (varies from 0.004 Å at 10000Å to 0.1 Å at 50000 Å).)

For the rest of the work, we considered the solar spectrum in the domain containing all the lines from Table 1. For clarity, we present in Fig.1 the solar spectrum whose wavelengths are between 5750Å and 6700 Å. The normalization of the solar spectrum is performed according to the following procedure: the continuum is estimated locally (in wavelength) and the intensities are normalized so that the continuum corresponds to the wavelengths, i.e., the continuum (baseline level of the spectrum without absorption lines) corresponds to unity (1.0) at all wavelengths. Continuity is preserved between the different parts of the spectrum (which means there is no discontinuity in the continuum). Local normalization is a spectral processing technique that consists of adjusting the spectrum intensity segment by segment, rather than globally over the entire spectral domain.

3. Adaptation of spectra to FEROS characteristics

A homogeneous parameterization of the vast ensemble of spectra obtained using the three high-resolution spectrographs of the European Southern Observatory (ESO): FEROS (Fiberfed Extended Range Optical Spectrograph, resolution up to R=48,000 (Kaufer *et al.*, 1999)), UVES (Ultraviolet and Visual Echelle Spectrograph, resolution reaching R=110,000 (Dekker *et al.*, 2000)), HARPS (High Accuracy Radial velocity Planet Searcher, maximum resolution of R=115,000 (Mayor *et al.*, 2003)) was performed within the framework of the AMBRE project (de Laverny et al., 2013). The parameterization analyses for each spectrographic database are detailed in references (de Pascale *et al.*, 2014; Worley *et al.*, 2016, 2012) for FEROS, HARPS and UVES, respectively.

In this work, we retained only the synthetic spectra covering the range of G-type star spectra, i.e., solar-type stars, from the grid used by Bado

4 For more information download/Atlas_IR.pdf see https://bass2000.obspm.fr/

et al., 2025 as well as the values of σ_0 (see equation 5). We have 31 spectra as a sample for this work whose stellar parameters are as follows: 4750 K ≤ T_{eff} ≤ 6000 K; 4.0 ≤ log(g) ≤ 4.5; -0.5 dex ≤ [M/H] ≤ 0.5 dex and 0.0 dex ≤ [α/Fe] ≤ 0.2 dex. Where T_{eff} is the effective temperature (in Kelvin) that a black body would have with the same total luminosity and the same radius as the star, log(g) is the surface gravity (acceleration at the stellar surface) generally expressed as a decimal logarithm, [M/H] is the abundance fraction of elements with atomic number Z > 2 (i.e., heavier than hydrogen and helium) in stellar photospheres. The alpha-abundances ([α/Fe])–oxygen, neon, magnesium, silicon, sulfur, argon, calcium and titanium–,[M/H] and [α/Fe] are expressed in logarithmic units (decimal exponent, dex).

Thus, in total, 31 spectra meeting the aforementioned conditions constituted our sample of synthetic spectra for the estimation of σ_0 on one hand. Since the resolution of the real solar spectrum is very high compared to that of the FEROS spectrograph, we reduced the resolution of the solar spectrum to that of the FEROS instrument. Next, we apply the same procedures to the real solar spectrum for the estimation of σ_{CC}. The following steps were adopted:

- convolution with (R = 48000);
- resampling following the wavelength steps of 0.003 and 0.006 nm corresponding to the two reduction modes of the FEROS spectrograph;
- convolution with the rotational profile taking into account the rotational velocity and varying the center-to-limb darkening.
- determination of the full width at half maximum of the Cross-Correlation (see Eq. 3).

We retained 5 center-to-limb coefficient values between the value used by Bado *et al.*, 2025 and 1 for the mask closest to the solar stellar

parameters. After these steps, we obtain two solar spectra adapted to the different possible observation configurations by FEROS.

II. Estimation of line broadening and rotationa l velocities of feros synthetics and solar spectra

In this section, we give the main steps for determining the rotational velocities of the parameterized FEROS spectra from ESO (see Bado *et al.*, 2025 for more details). We evaluated the value of the rotational broadening corresponding to G-type stellar spectra. The impact of the center-to-limb darkening coefficient on the solar spectrum was analyzed by varying this parameter (see Sect. IV). The estimation of these rotational velocities was performed according to the following methodology:

1. Measurement of rotational broadening

Stellar rotation can be determined by different methods such as spectroscopy, photometry, asteroseismology and interferometry (see (Gray, 2008), for more details). In this work, we use spectroscopy but more precisely the cross-correlation function. The projected rotational velocity (Vsin(i)) corresponds to the product of the equatorial rotational velocity (V) of the star by the sine of the inclination angle i between the star's rotation axis and the observer's line of sight. The determination of Vsin(i) is based on the analysis of spectral line broadening due to the Doppler effect induced by the rotation of the stellar surface. For a spectrum emitted ($S_{emis}(\lambda)$) by a stellar surface in the absence of rotation, the real spectrum ($S_{reel}(\lambda)$) of this same rotating star is given by equation 1:

$$S_{reel}(\lambda) = S_{emis}(\lambda) * G(\lambda) \quad \textbf{(1)}$$

where G(λ) represents the rotational broadening function, defined by equation 2:

$$G(\lambda) = \frac{2(1-\varepsilon)\left[1-(\Delta\lambda/\Delta\lambda_L)^2\right]^{1/2}+\frac{\pi\varepsilon}{2}\left[1-(\Delta\lambda/\Delta\lambda_L)^2\right]}{\pi\Delta\lambda_L(1-\varepsilon/3)} \quad \textbf{(2)}$$

where ε is the center-to-limb darkening, $\Delta\lambda_L$ represents the maximum broadening and $\Delta\lambda = \lambda V\sin(i)/c$. The center-to-limb darkening coefficients were extracted from the atmospheric models of (Claret, 2000)**.** A grid of 19 Vsin(i) values, sampled between 0 and 100 km/s, was defined to ensure optimal coverage of the observed stellar rotational parameter space. This systematic approach enabled the calibration of the parameter σ_0.

2. Calculation of the cross-correlation function (CC) and derivation of the coupling constant

To estimate the rotational velocity of a star from its spectrum S(λ), we perform a cross-correlation (CC) of the spectrum with specific binary masks M(λ) in order to obtain the correlation function (Melo *et al.*, 2001; Recio-Blanco *et al.*, 2004; Weise *et al.*, 2010) defined according to equation 3:

$$CC(\lambda) = \int_0^\infty S_{reel}\,(\lambda).M(\lambda)d\lambda \quad \textbf{(3)}$$

The masks M(λ) are composed of narrow lines and are generated from theoretical spectra representing the absorption lines expected for a given stellar type. These masks allow the elimination of unreliable spectral regions and act as a filter. The cross-correlation function (CC) is then fitted by a Gaussian function, which allows the determination of its characteristic width defined by equation 4:

$$\sigma_{CC} = \frac{FWHM_{CC}}{2\sqrt{2ln2}}, \quad \textbf{(4)}$$

where $FWHM_{CC}$ is the full width at half maximum of CC(λ). We integrated over a wide velocity domain of ±500 km/s, with a velocity step ΔV∼2.22 km/s and 4.44 km/s for a wavelength step of 0.003 nm and 0.006 nm, respectively. Once this broadening is deduced from the

Gaussfit function[5] providing the precision as well as the associated errors, a calibration of equation 5 follows to determine the coupling constant A when we apply it to real spectra. This total broadening is defined by:

$$V_{broad} = A\sqrt{(\sigma_{CC}^2 - \sigma_0^2)} \quad \textbf{(5)}$$

where σ_{CC} is the line width of the real spectrum and σ_0 results from the intrinsic width of the lines (i.e., for a star without rotation). In practice, A and σ_0 are deduced from the simulation of synthetic spectra. V_{broad} quantifies the mean broadening of these lines. This broadening is an observational parameter that quantifies the total measured width of spectral lines, regardless of its physical origin. This broadening results from multiple physical processes within stellar atmospheres, including: projected rotational velocity (Vsin(i)), macroturbulence velocity (Vmacro) and microturbulence velocity (Vmicro). For the majority of stars, V_{broad} is primarily influenced by Vsin(i) when the latter exceeds a few km/s, namely 2-4 km/s, particularly for slow rotators (Gray, 2008; Reiners and Schmitt, 2003).

III. Effect of the center-to-limb coefficient on synthetic spectra: G spectral types

In order to determine the influence of the limb-darkening coefficient on rotational broadening, we applied equation 6:

$$G(\lambda) = \frac{2(1-\varepsilon_i)\left[1-(v/Vb)^2\right]^{1/2} + \frac{\pi\varepsilon}{2}\left[1-(v/Vb)^2\right]}{\pi Vb(1-\varepsilon_i/3)} \quad \textbf{(6)}$$

by setting $\Delta\lambda_L = \lambda Vb/c$ and $\Delta\lambda/\lambda = v/c$ where v in Equ.2 and Vb represents V_{broad}.

We present in Fig.2 a portion (for clarity) of the solar spectrum at a resolution of 48,000 before applying the CC. At this stage of instrumental convolution, the instrumental broadening corresponds to

5 For more details on the Gaussfit function, see: https://www.nv5geospatialsoftware.com/docs/GAUSSFIT.html

rotational broadening of approximately 6.25 km/s in the visible domain, which significantly affects rotation velocity measurements for slow rotators since it is independent of stellar motion.

1. Line selection

The determination of spectral broadening requires the selection of well-defined and stable absorption lines. The choice of these specific lines serves as a reference for Doppler shift measurements; avoids contamination from regions containing telluric lines–to avoid regions heavily contaminated by Earth's atmosphere, cosmic, or instrumental artifacts; and optimizes the signal to maximize the contrast of these lines and minimize noise that is, avoiding lines sensitive to stellar activity (chromospheric emission).

Table 1 . Table presenting the different wavelength regions used for spectral analysis.

Region	λmin (nm)	λmax (nm)	Region	λmin (nm)	λmax (nm)
1	666	673	10	458.5	467
2	565.5	572.5	11	450.5	458
3	539	543	12	440.5	449.2
4	526	532	13	430	440.5
5	512	519	14	424.5	430
6	499	505.5	15	414	422
7	491	496	16	407.5	414
8	480	489	17	401.9	407.5
9	467.4	474	N/A	N/A	N/A

Table 1 presents the wavelength intervals of different spectral regions used for stellar spectroscopic analysis. These regions define the portions of the spectrum used for cross-correlation (CC) calculations.

The more numerous and well-defined the lines in these regions, the more accurate the resulting CC will be. Thus, the broadening of the CC reflects stellar macroturbulence, stellar rotation, and instrumental effects.

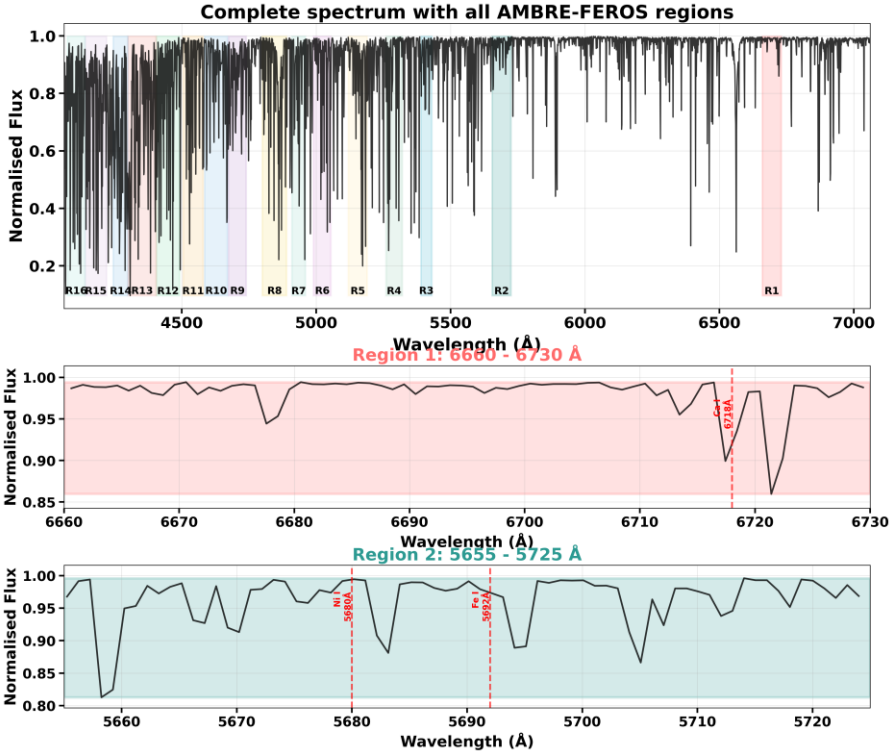

Figure 1 : Solar spectrum with all AMBRE-FEROS regions. *

For clarity, only the first two regions from Table 1 are presented (second and third pannels). The lines identified in these regions are respectively those of Calcium (Ca I at 6718 Å, R1); Iron (Fe I at 5692 Å, R2) and Nickel (Ni I at 5680 Å, R2).

These regions cover key spectral features, such as the magnesium triplet around 516 nm, H_β(486,1 nm), H_γ(434,1 nm), H_δ(410,1 nm), as well as spectral signatures of numerous atomic elements. This wealth of information provides sufficient sensitivity to cover the range of required

stellar parameters. These regions span from the near UV(∼380-400 nm) to the red(∼650-680 nm), covering a broad portion of the visible spectrum. This reflects the fact that we used only limb-darkening coefficients covering the visible domain. Indeed, this coverage allows exploitation of different types of lines with variable sensitivities to stellar parameters. This distribution favors regions with metallic lines (the most informative) for solar-type stars.

2. Application of CC to the Solar Spectrum

We apply CC to the real spectrum using the mask closest to its stellar parameters. The parameter values for the used mask are respectively T_{eff} = 5750 K; log(g) = 4.5; [M/H] = 0.0 dex and [α/Fe] = 0.0dex; for the Sun T_{eff} = 5780 K; log(g) = 4.5; [M/H] = 0.0 dex and [α/Fe] = 0.0 dex (Asplund *et al.*, 2009). During the estimation of the CC width, the function used stores the reduced χ^2 statistic value, which is used to evaluate the quality of the Gaussian fit. The χ^2 is estimated and represents an objective measure of fit quality, essential for validating the relevance of the Gaussian model for spectral data. For this purpose, we established the following criteria to validate the fit:

- the contrast must be strictly negative, thus ensuring an absorption profile
- the error on the amplitude must be less than 20% of the amplitude value, ensuring that the CC profile significantly dominates the noise.

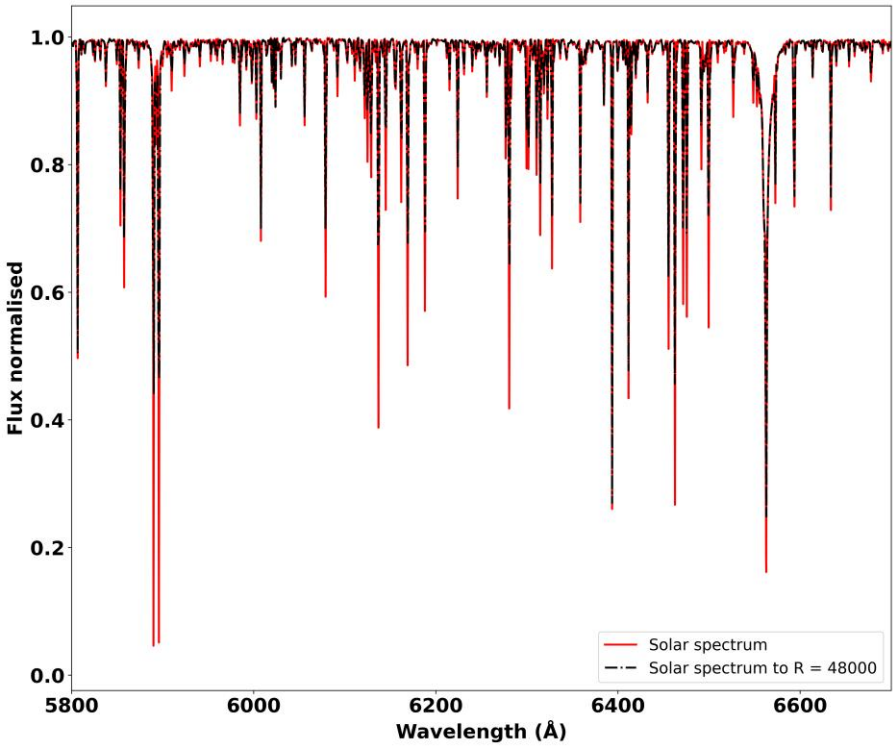

Figure 2 : Adaptation of the solar spectrum from Fig. 1 to the resolution of the FEROS spectrograph (black dotted line).

At FEROS resolution, we note a decrease in line depth. For clarity, we have not shown the two regions R1 and R2.

The profile amplitude (multiplied by 100, expressed as a percentage) is defined by the maximum height of the Gaussian, while the contrast is a measure that compares the depth of the absorption (or emission) line relative to the continuum (background level of the spectrum). If the contrast is positive, this indicates a poor fit (the Gaussian is inverted). CCs satisfying these conditions were considered well-defined. We present the CC results in Table 2. For the calculation of V_{broad} we consider the slope A = 1.89±0,01; $FWHM_0$ = 12.746±0.113 derived by Bado *et al.*, 2025.

IV. Discussion

Our measurements reveal a significant increase in $FWHM_{CC}$ widths as a function of the limb-darkening coefficient applied during cross-correlation with the mask closest to the Sun's parameters (see Table 2). This implies greater broadening of the CC Gaussian when the limb-darkening coefficient increases, and consequently V_{broad} increases. A broader $FWHM_{CC}$ often signifies faster motions in the solar plasma (V_{broad} increases) (Grassitelli *et al.*, 2016). This variability demonstrates the complexity of physical processes affecting spectral line profiles in stellar atmospheres. Furthermore, this variation (44.8%) suggests a physical effect related to the observational geometry, as limb darkening results from the variation of optical depth (denoted τ, which measures the cumulative opacity of a medium) depending on the viewing angle. At the center of the stellar disk, the perpendicular line of sight probes the deep, hot photospheric layers, while at the limb, the oblique geometry allows observation of only the cooler superficial layers, both corresponding to $\tau \approx 2/3$ which defines the visible photosphere.

Table 2 : Evolution of line width ($FWHM_{CC}$) and associated velocity (V_{broad}) with the limb-darkening correction coefficient

ε_i	$FWHM_{CC}$	err_{FWHMCC}	cont	err_{cont}	quality	$FWHM_0$	err_{FWHM0}	V_{broad}
	(km/s)	(km/s)				(km/s)	(km/s)	(km/s)
0,696	17,69	0,091	-9,787	0,023	$3{,}1\times10^{-4}$	12,746	0,113	9,85
0,772	19,271	0,134	-30,301	0,057	$4{,}9\times10^{-4}$	12,746	0,113	11,6
0,848	19,743	0,194	-29,623	0,08	$2{,}4\times10^{-4}$	12,746	0,113	12,1
0,924	21,404	0,151	-28,67	0,058	$3{,}1\times10^{-4}$	12,746	0,113	13,8
1	21,863	0,219	-28,13	0,081	$2{,}7\times10^{-4}$	12,746	0,113	14,26

(Claret, 2000) stipulates that limb-darkening coefficients depend on the stellar parameters of the star and consequently for solar-type stars an optimal coefficient of 0.7 is best suited. The value used by Bado *et al.*,

2025 is 0.696 (see Table 2). The measured V_{broad} of 9.85 km/s for the Sun, which is a G-type star, falls within the expected intermediate range, higher than late K stars but lower than more massive F stars. The limb darkening observed in stellar atmospheres results from the variation of temperature and density with optical depth (Claret, 2000; Gray, 2008). Stars appear darker at their limb than at the center of their disk because we observe the higher and cooler layers of stellar photospheres. This intensity variation directly influences rotation velocity measurements obtained through cross-correlation. Indeed, by applying the limb-darkening coefficient, we simulate the observation of different parts of the stellar disk.

Our results from Table 2 show that the choice of limb-darkening coefficient can introduce substantial systematic uncertainty on the measured widths and therefore on the estimation of rotation velocity V_{broad}. To minimize these effects, we recommend using empirically determined limb-darkening coefficients for each spectral type and observational wavelength (see (Claret, 2000)).

Although Vsin(i) and V_{broad} are often used interchangeably, the broadening velocity (V_{broad}) represents an observational measurement that integrates all broadening mechanisms. These mechanisms include stellar rotation (Vsin(i)), macroscopic turbulence (generated by convective motions or pulsations), instrumental broadening (determined by the spectrograph resolution), the influence of magnetic fields, and thermal broadening. Subsequently, we consider the rotational broadening value derived by Bado *et al.*, 2025.

Instrumental Broadening Correction

The instrumental broadening of FEROS generally follows a Gaussian profile with the spectral resolution R defined as $R = \lambda/\Delta\lambda$. For a moving source, the Doppler effect gives $\Delta\lambda/\lambda = v/c$ where c is the speed of light in vacuum and v represents the smallest velocity difference that the instrument can resolve. We then obtain $v = c/R$. For FEROS (R = 48,000), v = 6.25 km/s. For a Gaussian profile, this criterion corresponds exactly to a separation equal to $FWHM_{inst}$. Then σ_{inst} =

$FWHM_{inst}/\sqrt{2(2ln2)}$. The resulting intrinsic stellar rotation is given by:

$$V_{Sol} = \sqrt{(Vbroad^2 - v^2)} = 7.61\, km/s \quad \textbf{(7)}$$

We note that instrumental broadening effectively contributes additively to the observed spectral broadening. Considering the other values from Table 2, we obtain respective V_{Sol} values of 9.78, 10.36, 12.30, and 12.81 km/s.

Effects of Macroturbulence and Microturbulence

The value of 7.61 km/s (see Eq.7) contains additional broadenings related to the other mechanisms mentioned previously. According to the works of (Díaz *et al.*, 2011; Dos Santos *et al.*, 2016; Foy, 1978; Gray, 2008)**,** the macroturbulence velocity (Vmac) increases with optical depth within the stellar atmosphere. Furthermore, the mean macroturbulence velocity also increases with the effective temperature of stars. For the Sun, the reference values typically adopted for (Vmac) are around 3 to 4 km/s, while the microturbulence velocity (Vmic) is estimated at approximately 1 km/s. Microturbulence is related to small-scale convection while macroturbulence is a large-scale motion. Macroturbulence contributes significantly to the broadening of solar spectral lines. (Glebocki and Gnacinski, 2005) published a catalog of Vsin(i) and the methods used for estimating these Vsin(i) are as follows: line width (LW), full width at half maximum measurements (FWHM), line profile convolution (CONV), cross-correlation function analysis (C-C), Fourier transform line profile analysis (FTLP). This catalog presents data collected from various sources and observations from several publications and reports Vsin(i) values for the Sun of 2.2±0.7 km/s (FTLP); 1.1±0.6 km/s (C-C) and 2±0.3 km/s (Conv), respectively. In addition to the differing methods, it should be noted that the spectrographs used do not have the same resolutions.

Conclusion

This study has allowed us to quantify the impact of limb darkening on spectral line profiles in G-type stars, revealing significant effects that must be taken into account in modern spectroscopic analysis. Our results demonstrate that limb darkening induces systematic variations in the intensity and full width at half maximum of the cross-correlation function ($FWHM_{CC}$). This study has enabled us to quantify the impact of limb darkening on spectral line profiles in G-type stars, revealing significant effects that must be taken into account in modern spectroscopic analysis. Our results demonstrate that limb darkening induces systematic variations in the intensity and width of spectral lines, with a more pronounced impact on strong lines than on weak lines. Hydrogen lines (Balmer series) and metallic lines show differential responses to this effect, confirming the dependence as a function of formation depth in the stellar atmosphere.

The analysis of the evolution of velocity V_{broad} as a function of the limb-darkening correction coefficient ϵi reveals a significant positive correlation. The results show that V_{broad} systematically increases from 9.85 km/s for ε_i = 0.696 to 14.26 km/s for ε_i= 1, representing a variation of 44.8%. This quasi-linear progression of V_{broad} with ε_i confirms the direct impact of limb darkening on stellar velocity measurements. The increase in broadening V_{broad} reflects the progressive broadening of spectral lines when the limb-darkening effect becomes more pronounced, which is consistent with theoretical stellar atmosphere models.

The observed relation (ε_i) exhibits a mean gradient of ∼10.3 km/s per unit of ε_i , suggesting that limb-darkening corrections can introduce non-negligible systematic biases in stellar velocity measurements. These results emphasize the necessity of systematically integrating limb-darkening corrections into spectroscopic analysis pipelines, particularly for G-type stars where this effect is most pronounced. Indeed, this is confirmed by Neilson and Lester, 2010 through limb-darkening coefficients derived based on the spherical PHOENIX atmosphere model, in which the optical structure changes rapidly for

these stellar types. Complementary studies using ATLAS and PHOENIX models confirm that the coefficients vary significantly for these stars, in relation to T_{eff}, log(g) and microturbulence, which justifies rigorous consideration during spectral analyses (Claret, 2017).

The perspectives opened by this study include extension to other spectral types, investigation of temporal effects related to stellar activity, and integration of these corrections into automated spectroscopic analysis pipelines. This research emphasizes the importance of considering geometric effects in the interpretation of stellar spectra and paves the way for more refined analyses of stellar atmosphere physics.

References

Asplund, M., Grevesse, N., Sauval, A.J., Scott, P., 2009. The Chemical Composition of the Sun. Annu. Rev. Astron. Astrophys. 47, 481–522. https://doi.org/10.1146/annurev.astro.46.060407.145222

Aufdenberg, J.P., Ludwig, H. -G., Kervella, P., 2005. On the Limb Darkening, Spectral Energy Distribution, and Temperature Structure of Procyon. ApJ 633, 424–439. https://doi.org/10.1086/452622

Bado, F., Laverny, P. de, Kam, Z., Recio-Blanco, A., Palicio, P.A., Koulidiati, J., 2025. The AMBRE Project: Line-broadening and stellar rotation of ESO/FEROS archived spectra. A&A 704, A49. https://doi.org/10.1051/0004-6361/202557176

Claret, A., 2017. Limb and gravity-darkening coefficients for the TESS satellite at several metallicities, surface gravities, and microturbulent velocities. A&A 600, A30. https://doi.org/10.1051/0004-6361/201629705

Claret, A., 2000. A new non-linear limb-darkening law for LTE stellar atmosphere models. Calculations for -5.0 <= log[M/H] <= +1,

2000 K <= Teff <= 50000 K at several surface gravities. Astronomy and Astrophysics 363, 1081–1190.

Collins, G.W., Ii, Truax, R.J., 1995. Classical rotational broadening of spectral lines. ApJ 439, 860. https://doi.org/10.1086/175225

Curdt, W., 2001. The SUMER spectral atlas of solar-disk features, in: AIP Conference Proceedings. Presented at the SOLAR AND GALACTIC COMPOSITION: A Joint SOHO/ACE Workshop, AIP, Bern (Switzerland), pp. 45–46. https://doi.org/10.1063/1.1433977

de Laverny, P., Recio-Blanco, A., Worley, C.C., De Pascale, M., Hill, V., Bijaoui, A., 2013. The AMBRE Project: Stellar Parameterisation of ESO Archived Spectra. The Messenger 153, 18–21.

De Laverny, P., Recio-Blanco, A., Worley, C.C., Plez, B., 2012. The AMBRE project: A new synthetic grid of high-resolution FGKM stellar spectra. A&A 544, A126. https://doi.org/10.1051/0004-6361/201219330

De Pascale, M., Worley, C.C., De Laverny, P., Recio-Blanco, A., Hill, V., Bijaoui, A., 2014. The AMBRE project: Parameterisation of FGK-type stars from the ESO:HARPS archived spectra. A&A 570, A68. https://doi.org/10.1051/0004-6361/201423767

Dekker, H., D'Odorico, S., Kaufer, A., Delabre, B., Kotzlowski, H., 2000. Design, construction, and performance of UVES, the echelle spectrograph for the UT2 Kueyen Telescope at the ESO Paranal Observatory, in: Iye, M., Moorwood, A.F.M. (Eds.), . Presented at the Astronomical Telescopes and Instrumentation, Munich, Germany, p. 534. https://doi.org/10.1117/12.395512

Díaz, C.G., González, J.F., Levato, H., Grosso, M., 2011. Accurate stellar rotational velocities using the Fourier transform of the cross correlation maximum. A&A 531, A143. https://doi.org/10.1051/0004-6361/201016386

Dos Santos, L.A., Meléndez, J., Nascimento, J.-D.D., Bedell, M., Ramírez, I., Bean, J.L., Asplund, M., Spina, L., Dreizler, S., Alves-Brito, A., Casagrande, L., 2016. The Solar Twin Planet Search: IV. The Sun as a typical rotator and evidence for a new rotational braking law for Sun-like stars⋆⋆⋆. A&A 592, A156. https://doi.org/10.1051/0004-6361/201628558

Doyle, A.P., Davies, G.R., Smalley, B., Chaplin, W.J., Elsworth, Y., 2014. Determining stellar macroturbulence using asteroseismic rotational velocities from Kepler. Monthly Notices of the Royal Astronomical Society 444, 3592–3602. https://doi.org/10.1093/mnras/stu1692

Espinoza, N., Jordán, A., 2015. Limb darkening and exoplanets: testing stellar model atmospheres and identifying biases in transit parameters. Monthly Notices of the Royal Astronomical Society 450, 1879–1899. https://doi.org/10.1093/mnras/stv744

Foy, R., 1978. A study of the microturbulence in giants in terms of stellar evolution. Astronomy and Astrophysics 67, 311–321.

Glebocki, R., Gnacinski, P., 2005. VizieR Online Data Catalog: Catalog of Stellar Rotational Velocities (Glebocki+ 2005). VizieR Online Data Catalog 3244, III/244.

Grassitelli, L., Fossati, L., Langer, N., Simón-Díaz, S., Castro, N., Sanyal, D., 2016. Metallicity dependence of turbulent pressure and macroturbulence in stellar envelopes. A&A 593, A14. https://doi.org/10.1051/0004-6361/201628912

Gray, D.F., 2008. The Observation and Analysis of Stellar Photospheres, The Observation and Analysis of Stellar Photospheres.

Gustafsson, B., Edvardsson, B., Eriksson, K., Jørgensen, U.G., Nordlund, Å., Plez, B., 2008. A grid of MARCS model atmospheres for late-type stars: I. Methods and general

properties. A&A 486, 951–970. https://doi.org/10.1051/0004-6361:200809724

Hayek, W., Sing, D., Pont, F., Asplund, M., 2012. Limb darkening laws for two exoplanet host stars derived from 3D stellar model atmospheres: Comparison with 1D models and HST light curve observations⋆. A&A 539, A102. https://doi.org/10.1051/0004-6361/201117868

Howarth, I.D., 2011. On stellar limb darkening and exoplanetary transits: Limb darkening and exotransits. Monthly Notices of the Royal Astronomical Society 418, 1165–1175. https://doi.org/10.1111/j.1365-2966.2011.19568.x

Kaufer, A., Stahl, O., Tubbesing, S., Nørregaard, P., Avila, G., Francois, P., Pasquini, L., Pizzella, A., 1999. Commissioning FEROS, the new high-resolution spectrograph at La-Silla. The Messenger 95, 8–12.

Manduca, A., Bell, R.A., Gustafsson, B., 1977. Limb darkening coefficients for late-type giant model atmospheres. Astronomy and Astrophysics 61, 809–813.

Mayor, M., Pepe, F., Queloz, D., Bouchy, F., Rupprecht, G., Lo Curto, G., Avila, G., Benz, W., Bertaux, J.-L., Bonfils, X., Dall, Th., Dekker, H., Delabre, B., Eckert, W., Fleury, M., Gilliotte, A., Gojak, D., Guzman, J.C., Kohler, D., Lizon, J.-L., Longinotti, A., Lovis, C., Megevand, D., Pasquini, L., Reyes, J., Sivan, J.-P., Sosnowska, D., Soto, R., Udry, S., van Kesteren, A., Weber, L., Weilenmann, U., 2003. Setting New Standards with HARPS. The Messenger 114, 20–24.

Melo, C.H.F., Pasquini, L., De Medeiros, J.R., 2001. Accurate $V\sin i$ measurements in M 67: The angular momentum evolution of 1.2 $M_\odot$ stars. A&A 375, 851–862. https://doi.org/10.1051/0004-6361:20010897

Neilson, H.R., Lester, J.B., 2010. Using Limb-Darkening to Measure the Masses of Red Giants. https://doi.org/10.48550/ARXIV.1011.4387

Recio-Blanco, A., Piotto, G., Aparicio, A., Renzini, A., 2004. Rotation velocities of hot horizontal branch stars in the globular clusters NGC 1904, NGC 2808, NGC 6093, and NGC 7078: The database. A&A 417, 597–604. https://doi.org/10.1051/0004-6361:20040003

Reiners, A., Schmitt, J.H.M.M., 2003. Rotation and differential rotation in field F- and G-type stars. A&A 398, 647–661. https://doi.org/10.1051/0004-6361:20021642

Weise, P., Launhardt, R., Setiawan, J., Henning, T., 2010. Rotational velocities of nearby young stars. A&A 517, A88. https://doi.org/10.1051/0004-6361/201014453

Worley, C.C., De Laverny, P., Recio-Blanco, A., Hill, V., Bijaoui, A., 2016. The AMBRE Project: Stellar parameterisation of the ESO:UVES archived spectra. A&A 591, A81. https://doi.org/10.1051/0004-6361/201526814

Worley, C.C., De Laverny, P., Recio-Blanco, A., Hill, V., Bijaoui, A., Ordenovic, C., 2012. The AMBRE Project: Stellar parameterisation of the ESO:FEROS archived spectra. A&A 542, A48. https://doi.org/10.1051/0004-6361/201218829